Interpretation of the optical absorption spectrum of uranium germanate

1993 J. Phys.: Condens. Matter 5 9223

(http://iopscience.iop.org/0953-8984/5/49/024)

J. Phys.: Condens. Matter 5 (1993) 9223–9234. Printed in the UK

Interpretation of the optical absorption spectrum of uranium germanate

Z Gajek†‖, J C Krupa†, Z Żołnierek‡, E Antic-Fidancev§ and M Lemaitre-Blaise§

† Laboratoire de Radiochimie, Institut de Physique Nucléaire, 91406 Orsay Cédex, France
‡ W Trzebiatowski Institute of Low Temperature and Structure Research, Polish Academy of Sciences, 50–950 Wrocław, PO Box 937, Poland
§ UPR 210, CNRS, 1 Place A Briand, 92195 Meudon Cédex, France

Received 6 July 1993, in final form 25 August 1993

Abstract. Visible and infrared absorption spectra of U^{4+} in $UGeO_4$ are described and interpreted in terms of the standard parametrization scheme. One of the two models considered is consistent with available interpretations of other uranium germanates and silicates. The second one originating from theoretical estimation of the crystal-field effect permits exceptional properties of the compound under consideration, in particular, an untypical assignation of the electronic energy levels and values of the crystal-field parameters in comparison with other tetragonal oxides.

1. Introduction

A variety of crystal-field (CF) effects generated on the U^{4+} ion by similar tetragonal germanate and silicate matrices [1–3] or a controversy reappearing recently concerning the crystal-field strength in the simple actinide dioxides [4] point to a complex nature of the actinide–oxygen bond. Investigation of new materials is an important way for a better recognition of the problem.

The uranium germanate, $UGeO_4$, an easily preparable compound, seems to be the best candidate for this aim. So far, it is the only uranium oxide that crystallizes with the scheelite-type structure ($CaWO_4$). We report here optical absorption measurements on a polycrystalline sample recorded in both the visible and infrared regions at various temperatures. The spectra obtained are interpreted in terms of the standard parametrization model. We are guided by the results of the latest spectroscopic studies on U^{4+} doped in similar tetragonal matrices [2, 3, 5] on the one hand, and independent theoretical predictions of the crystal-field effect based on both the angular overlap model (AOM) [6] and *ab initio* calculation [7] methods on the other.

2. Experimental details

$UGeO_4$ was obtained by heating in an evacuated quartz ampulla a stoichiometric mixture of UO_2 and GeO_2 in the desired proportion. After 24 h of heating at 950 °C we obtained

‖ On leave from W Trzebiatowski Institute of Low Temperature and Structure Research, Polish Academy of Sciences, 50–950 Wrocław, PO Box 937, Poland.

0953-8984/93/499223+12$07.50

light green powder of $UGeO_4$. X-ray analysis has shown the product to be a single phase that could be indexed in the I-centred tetragonal system $I4_1/a$ with the lattice parameters $a = 5.071$ Å and $c = 11.290$ Å. Our crystallographic data are in good agreement with those reported previously by Durif [8].

The optical absorption spectra of the polycrystalline samples mixed with powdered KBr were obtained from 2600 to 400 nm at 300 and 9 K using a Cary model 2400 spectrophotometer. Besides, the absorption spectra in the range 750–400 nm were recorded at 4.2, 100 and 300 K with a high-resolution Jobin Yvon HR 1000 spectrometer equipped with a Hamamatsu R374 photomultiplier and a 1200 g mm^{-1} grating.

3. Preliminary estimation of the crystal-field effect

The exact point symmetry at the uranium site in $UGeO_4$ is S_4. Eight oxygens surrounding the metal ion are arranged in two interpenetrating tetrahedra twisted mutually by a 94.98° angle. The deviation from the approximate D_{2d} symmetry is measured by the departure of the above angle from the ideal 90° value. The metal–ligand (ML) distance R and the angle θ between the S_4 axis and the metal–ligand bond for both the tetrahedra are compared in table 1 with those of other silicate and germanate matrices of the zircon, thorite and scheelite structures. As seen, the elongated tetrahedron has remarkably shorter ML distance than the flattened one only for $UGeO_4$. The differences in the coordination geometry have considerable impact on the crystal-field parameters (CFP). This is well seen through the coordination factors W_{kq} used in the one-parameter version of the angular overlap model (AOM-1) [6]. These factors link the crystal-field parameters B_q^k with the AOM parameter e_σ in a very simple way:

$$B_q^k = W_{kq} e_\sigma .$$

Thus within the frame of the AOM-1 approximation the coordination geometry fully determines both the sign and relative value of the crystal-field parameters. The only adjustable parameter, e_σ, has a clear physicochemical meaning [6] and is a valuable measurement of the crystal-field strength. The W_{kq} factors have been calculated according to the following formula:

$$W_{kq} = \frac{2k+1}{7}\left[\begin{pmatrix} 3 & k & 3 \\ 0 & 0 & 0 \end{pmatrix}\right]^{-1} \sum_{\mu=0,\pm1} \begin{pmatrix} 3 & k & 3 \\ -\mu & 0 & \mu \end{pmatrix} \sum_t \left(\frac{R_0}{R_t}\right)^{\alpha_\mu} \left(\frac{e_\mu}{e_\sigma}\right) C_q^{k*}(t)$$

where t runs over ligands, $C_q^k(t) \equiv C_q^k(\theta_t, \phi_t)$ are the normalized spherical harmonics, R_t, θ_t, ϕ_t are the polar coordinates of ligand t, R_0 is a mean metal–ligand distance, $e_\mu \equiv e_\mu(R_0)$ stands for the effective AOM parameters $e_\sigma(\mu = 0)$ and $e_\pi(\mu = \pm 1)$ and α_μ is the power exponent determining the ML distance dependence of the actual $e_\mu(R_t)$ parameter. Both the e_μ/e_σ ratio and the α_μ exponents are characteristic for a given ML system. The values for the U^{4+}–O^{2-} ligator have been taken from [6].

The imaginary terms have been estimated to be very small and to have practically no influence on CF splitting, so they are not shown in table 1. The *ab initio* calculations based on a simple perturbative model (see below) in which the whole lattice contribution is taken into account also give negligible imaginary terms. This allows us to limit the discussion to the approximate D_{2d} symmetry group.

For all the compounds listed in table 1 the tetragonal parameter B_4^4 dominates and determines the global CF splittings. Accordingly the smallest CF effect should be observed just for $UGeO_4$ for which the W_{44} factor is less than one-third of its value for U^{4+}:$ZrSiO_4$.

Table 1. Comparison of the oxygen-ion coordinates and the AOM-I geometrical factors W_{kq}[a] for the various germanate and silicate crystals.

Matrix[b]	Tetrahedron[c]	R (Å)	θ (deg)	W_{20}	W_{40}	W_{44}	W_{60}	W_{64}
$ZrSiO_4$ [9]	el	2.436	32.90	−2.70	1.62	−7.02	−0.87	−0.04
	fl	2.057	74.74					
β-$ThGoO_4$ [10]	el	2.473	31.81	−0.12	1.14	−2.94	−1.41	0.16
zircon	fl	2.358	78.58					
α-$ThGeO_4$ [10]	el	2.332	39.31	0.49	−2.02	−2.86	−0.52	−1.64
scheelite	fl	2.353	69.37					
α-$ThSiO_4$ [11]	el	2.466	30.75	0.17	1.03	−1.76	−1.18	−0.01
thorite, low-temp. phase	fl	2.368	76.83					
$UGeO_4$ [8]	el	2.307	34.18	1.71	−1.13	−1.96	−1.05	−1.27
	fl	2.471	68.69					

[a] Calculated for $R_0 = 2.362$ Å—the averaged ML distance for all matrices.
[b] Crystalographic data from references indicated.
[c] el—elongated, fl—flattened.

Comparing the W_{kq} values for zircon and scheelite matrices, an inversion of the signs of B_0^2 and B_0^4 parameters and much higher B_4^6 parameters for the latter structure may be noticed.

Taking $e_\sigma = 1940\ cm^{-1}$, i.e. a value consistent with the CF interpretation for UO_2 [12] and U^{4+}:$ThSiO_4$ [2], and the W_{kq} factors from table 1 one obtains the CFP listed in table 2. These parameters have been used as a starting set in the fitting procedure described later. For comparison, the CFP obtained using the *ab initio* perturbative model [7] are also shown in table 2. The model is based on the perturbation expansion of the intra-ionic interaction in the subspace of free-ion eigenfunctions. Additionally, the electrostatic contribution of the whole lattice including the effect of induced electric dipoles is taken into account (see [7] for details).

Table 2. Crystal-field parameters estimated with the AOM-I approach in comparison with the results of the *ab initio* calculations for $UGeO_4$ (cm^{-1}).

	B_0^2	B_0^4	B_4^4	B_0^6	B_4^6
AOM-I	3324	−2199	−3816	−2040	−2469
ab initio	3998	−588	−3799	339	−1038

The theoretical results do not preserve the ratios of the CF parameters of the same order that are characteristic for AOM. The calculations show that the off-AOM contributions coming mainly from further neighbour point charges as well as the ligand polarization effects [6] play an important role in the case of $UGeO_4$. Nevertheless the leading terms, B_0^2 and B_4^4, are similar in both approaches.

4. Optical spectrum

The absorption spectra of $UGeO_4$ are shown in figures 1 and 2. One observes broad lines characteristic of solid compounds with large phonon sidebands. Some of them are too broad to be assigned to single electronic transitions, especially the puzzling bands near 15 338 and 15 774 cm^{-1}. Similar structures have been observed in this region for U^{4+}:α-$ThSiO_4$ [2] and U^{4+}:α-$ThGeO_4$ [5] (see figure 3). The polarized spectra of the above doped single

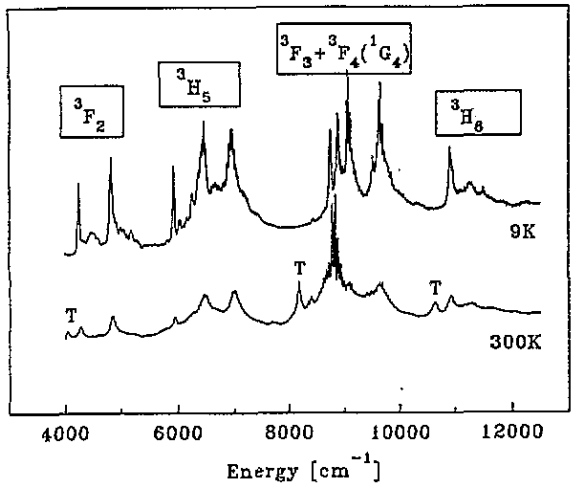

Figure 1. Absorption spectra of $UGeO_4$ at different temperatures in the infrared region.

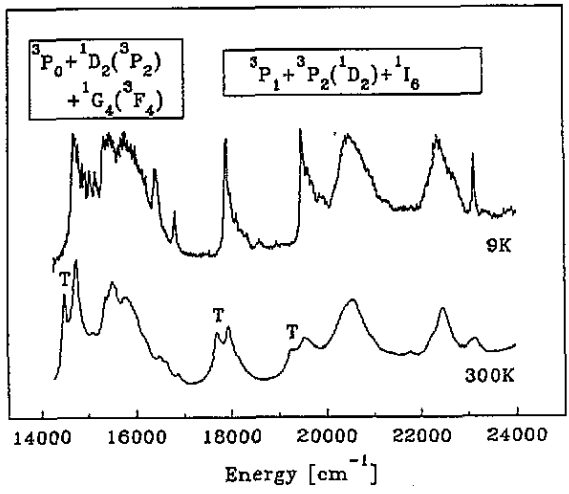

Figure 2. Absorption spectra of $UGeO_4$ at different temperatures in the visible region.

crystals have allowed one to distinguish and assign precisely particular lines of the bands. Therefore, the interpretation of the spectra of U^{4+}:$ThSiO_4$ [2] is believed to be a good starting point in the present study.

Twenty three bands of electronic origin have been recognized. The corresponding energies are listed in table 3 together with the energy gaps Δ_T and Δ_V from thermally induced peaks (see figure 1) and vibrational sidebands, respectively. They may be classified as follows (see figures 4 and 5):

(i) sharp lines corresponding to the transition to a separated single level or levels accidentally degenerate: 4246, 5914, 16812, 19499, 23127 cm^{-1};

(ii) transitions broadened slightly by vibrational sidebands of a neighbouring line or transitions to a few (two?) levels laying very close together: 4819, 8712, 8847, 10890, 16419, 17903 cm^{-1}:

(iii) complex structures consisting of several relatively sharp lines: 6458, 6945, 9030, 9604, 14696, 15338 cm^{-1};

(iv) broad bands: 15774, 20486, 22361 cm^{-1}; and

Table 3. Energies of the observed electronic transitions and the corresponding phonon sidebands and thermally induced transitions for $UGeO_4$ (cm^{-1}).

Energy	Intensity	Shape[a]	Δ_T	Δ_V
4246	1.44	(i)	229	~100, 177, 220, 275, 340, 447
4819	1.80	(ii)	235	91, 165, 214, 340, 450
5914	1.68	(i)		108, 165, 233, 324, 450
6458	2.31	(iii)		
6945	2.19	(iii)		
8394	0.90	(v)	239	
8712	2.17	(ii)		
8847	2.41	(ii)		
9030	3.04	(iii)		
9071	2.43	(iii)		
9490	1.63	(v)		
9604	2.62	(iii)		
10890	1.94	(ii)	276	
14696	1.78	(iii)	236	95, 175, 220, 333, 454
15338	1.82	(iii)		
15774	1.85	(iv)		
16419	1.61	(v)		
16812	1.36	(v)		
17903	1.80	(ii)	235	90, 175, 217, 316
19499	1.86	(i)	275	92, 173, 337, 417
20486	1.83	(iv)		
22361	1.82	(iv)		
23127	1.67	(i)		

[a] The lines are classified in five groups, (i)–(v), defined in the main text.

(v) less intense lines: 6240, 8394, 9490 cm^{-1}.

There are some doubts concerning the electronic origin of the lines at 6240 and 9490 cm^{-1}, since they lay in the region of phonon sidebands. Their intensities, however, are higher than that of other phonon-induced transitions.

The observed phonon sidebands reveal the expected regularity. Their maxima correspond to the following average phonon frequencies (cm^{-1}): 96, 172, 221, 275, 332 and 443 (see table 3), in reasonable agreement with the detailed study of the vibrational spectra of α-$ThGeO_4$ [13].

5. Two alternative interpretations

The conventional model Hamiltonian H describing ionic systems consists of two terms: the spherically symmetric, so-called 'free-ion' part H_0 and the crystal-field potential V. The 'free-ion' part, which in standard notation is written:

$$H_0 = \sum_{k=0,2,4,6} F^k f_k + \zeta_{5f} \sum_i l_i s_i + \alpha L(L+1) + \beta G(G_2) + \gamma G(R_7) + \sum_{k=0,2,4} M^k m_k + \sum_{k=2,4,6} P^k p_k$$

describes the Coulomb repulsion of the 5f electrons, their spin–orbit coupling and the higher-order corrections due to the configuration–interaction and relativistic effects [3]. The crystal-field potential in its usual form is expressed by:

$$V = \sum_{k,q,i} B_q^k C_q^k(i).$$

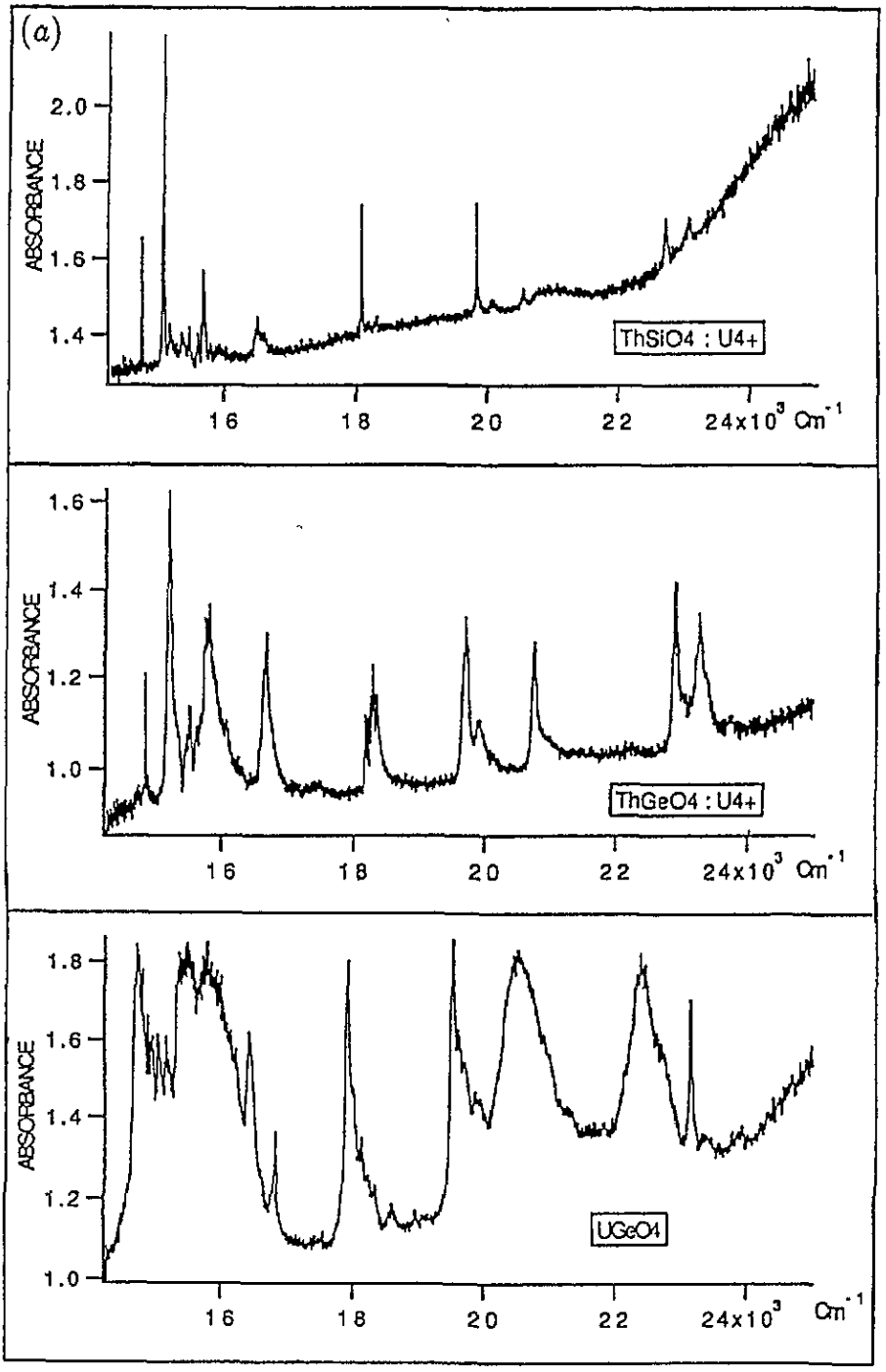
(a)
ABSORBANCE
2.0
1.8
1.6
1.4
ThSiO4 : U4+
16
18
20
22
24x10^3 Cm^-1
ABSORBANCE
1.6
1.4
1.2
1.0
ThGeO4 : U4+
16
18
20
22
24x10^3 Cm^-1
ABSORBANCE
1.8
1.6
1.4
1.2
1.0
UGeO4
16
18
20
22
24x10^3
Cm^-1

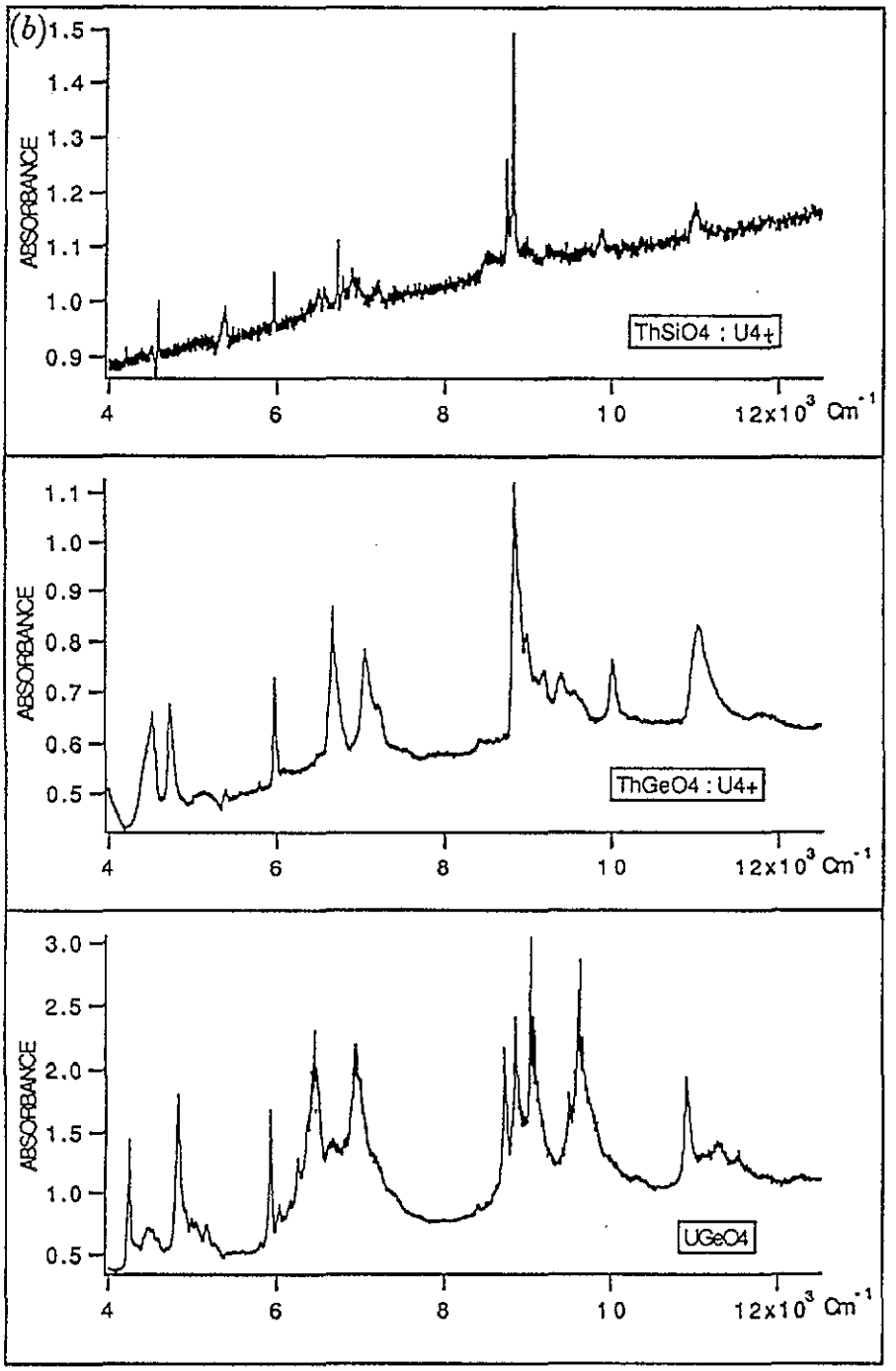

Figure 3. Absorption spectra of $UGeO_4$, U^{4+}:α-$ThSiO_4$ and U^{4+}:α-$ThGeO_4$ in the visible (*a*) and infrared (*b*) regions.

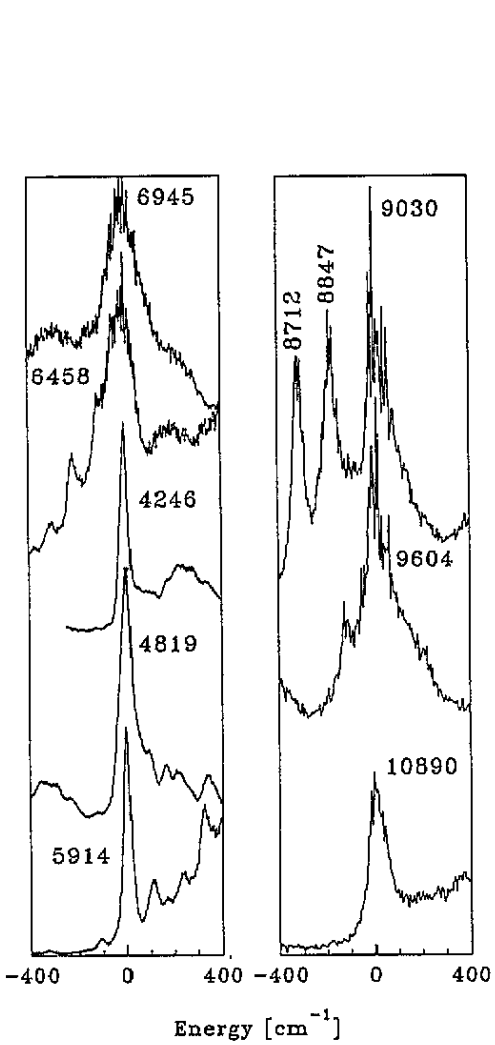

Figure 4. Comparison of the absorption bands in the infrared region.

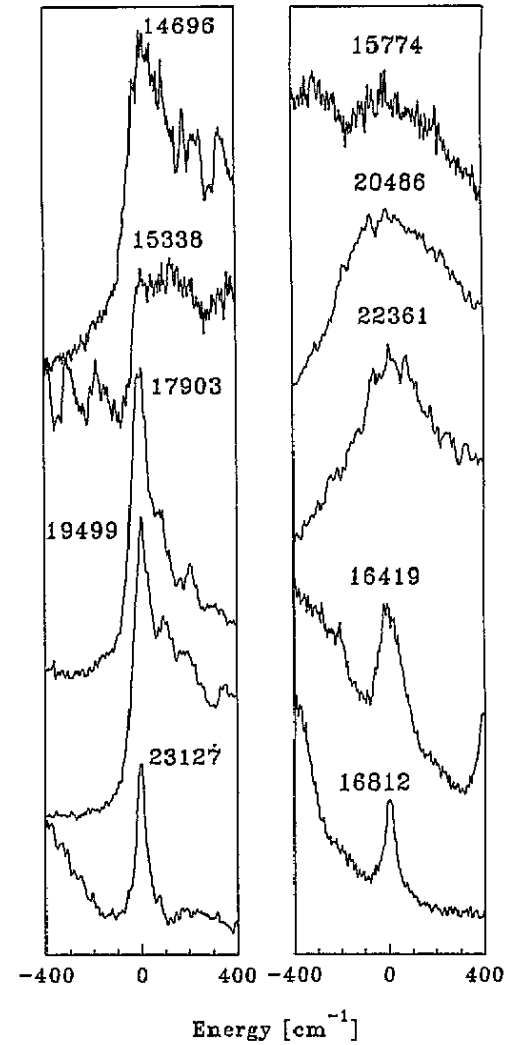

Figure 5. Comparison of the absorption bands in the visible region.

Fitting of the 14 'free-ion' parameters and five CF parameters of the model Hamiltonian to the observed electronic transitions would be practically impossible without additional assumptions. First the free-ion part is strongly believed to satisfy the general predictive model according to which there are some constant shifts of the parameters of the bonded ions in relation to their counterparts calculated from first principles for the actual free ions [3]. This gives good starting values of the main free-ion parameters F^k and ζ. The initial values and the relations between the higher-order free-ion parameters M^k and P^k were taken from [14].

Regarding the CF effect the following two independent approaches were applied: (a) approach based on similarity of the spectra of $UGeO_4$ and U^{4+}:$ThSiO_4$ in which the assignation of the most characteristic lines for U^{4+}:$ThSiO_4$ were preserved, and (b) interpretation based on the above AOM simulation of the CF potential. The latter method has

Table 4. Experimental and calculated energy levels of U^{4+} in $UGeO_4$ for two different assignations (cm^{-1}).

	Model (a)			Model (b)		
E_{obs}	Γ	E_{calc}	ΔE	Γ	E_{calc}	ΔE
0	4	0	0	1	19	19
				2	115	
235	5	151	−84	5	255	20
275	1	291	16	4	303	28
	2	1104		3	1126	
	1	1142		5	1341	
	3	1195		1	1458	
	5	1602				
4246	5	4270	24	5	4268	22
	3	4271		1	4394	
	4	4630				
4819	1	4837	18	4	4799	−20
	3	5630		3	5017	
	2	5849		2	5818	
5914	5	5900	−14	5	5852	−62
	4	6402		1	5898	
6458	5	6496	38	5	6180	
				3	6359	
6945	5	6926	−19	4	6892	−53
				5	6956	11
	2	7029		2	7028	
	1	7032				
	4	7576				
8394				3	8506	112
8712	5	8764	52	5	8718	6
8847	1	8874	27	4	8803	−44
	3	8897		2	8851	
9030	5	8939	−91	5	9068	38
	2	8961				
9071	5	9180	109	4	9094	23
	4	9304		1	9313	
9490				5	9364	−126
				1	9401	
	2	9521		3	9475	
9604	1	9693	89	5	9602	−2
	3	10012		2	9625	
	5	10103				
	1	10794				
	4	10957		4	10867	−23
10890	5	10980	90	5	10899	9
	3	11320		3	10909	
	4	11479		1	11113	
	5	11486		5	11341	
	3	11535		2	11341	
	2	11657		4	11396	
	1	11929		1	12454	
	5	12405		5	12551	
				3	12652	
				1	14558	
14696	1	14618	−78	5	14750	54
	3	14901		1	15380	
	4	14104		3	15402	

Table 4. (continued)

	Model (a)			Model (b)		
E_{obs}	Γ	E_{calc}	ΔE	Γ	E_{calc}	ΔE
15 338	1	15 267	−41	5	15 500	162
	5	15 385		4	15 523	
				1	15 695	
15 774	5	15 728	−46	4	15 917	143
	2	15 761		5	16 045	
	1	15 855		2	16 158	
				3	16 182	
16 419	1	16 464	45			
	4	16 574				
16 812	5	16 686	−126			
	3	17 271		1	16 928	
	2	17 359				
17 903	5	17 918	15	5	17 921	18
				4	17 993	
				3	18 003	
				2	18 705	
19 499	5	19 525	26	5	19 551	52
	3	19 553		1	20 284	
	1	19 582	83	2	20 383	
20 486	5	20 454	−33	5	20 444	−42
	4	20 529		3	20 458	
	2	20 537		1	21 186	
	5	20 982		5	21 506	
	1	21 116		4	21 605	
	3	21 597		5	21 738	
	4	21 998				
	3	22 453				
22 361	5	22 531	170	5	22 237	−124
	3	23 082		3	22 237	
23 127	1	23 214	−87	4	23 132	5

been proved to be adequate for a number of f-electron systems. One of the latest examples is a successful interpretation of the spectra of the low-symmetry actinide tetrafluorides [14, 16].

Within the D_{2d} approximate symmetry four different singlets Γ_1, Γ_2, Γ_3 and Γ_4 and one doublet Γ_5 are allowed. Assuming Γ_4 to be the ground state (like in U^{4+}:$ThSiO_4$ [2]) 36 transitions to Γ_1 and Γ_5 excited states are allowed by the electric dipole selection rules for the f^2 configuration below 25 000 cm^{-1}. At the beginning lines of type (i) and (ii) were considered only. They have been assigned like their counterparts for U^{4+}:$ThSiO_4$ and the crystal-field parameters were varied only. In the next steps the most intense components of the structures of type (iii), the maxima of the bands (iv), the less intense lines (v) and eventually two additional levels at 235 and 275 cm^{-1} deduced from the high-temperature spectra were successively taken into consideration. At the same time the number of varied parameters was increased. At the end 24 levels have been fitted with 13 independent parameters. The RMS error has been reduced to $\sim$ 100 cm^{-1}, which seems to be quite satisfactory taking into account the broadness of some of the lines and the reduced number of allowed transitions. The results of the fitting are shown in tables 4 and 5.

The AOM simulation leads to a different set of CF parameters and suggests another assignation of the observed lines. Following this approach, the Γ_1 singlet is a ground state and 33 transitions to Γ_4 and Γ_5 are allowed in the energy range of interest. Starting with

Table 5. Initial and final spectroscopic parameters obtained within the models (a) and (b) (cm^{-1}).

	Model (a)		Model (b)	
	Initial	Final	Initial	Final
F^2	42 918	42 920(265)	42 918	42 658(181)
F^4	39 873	39 129(519)	39 873	39 480(113)
F^6	25 588	27 753(584)	25 588	24 448(175)
ζ	1810	1767(12)	1810	1725(11)
α	30.1	22.0(0.2)	30.1	29.0(0.0)
β	−660	−899(6)	−660	−980(0)
γ		[1800]		[800]
P^{2a}	2715	493(177)	2715	1970(8)
M^{0b}		[0.77]		[0.77]
M^2		[0.43]		[0.43]
M^4		[0.29]		[0.29]
B_0^2	−1003	−1782(138)	3324	2918(37)
B_0^4	1147	2521(307)	−2199	−2051(19)
B_4^4	−2698	−3061(49)	−3816	−3026(7)
B_0^6	−2889	−3806(74)	−2040	−487(7)
B_4^6	−208	−504(294)	−2469	−1986(34)

[a] $P^4 = 0.5P^2$, $P^6 = 0.1P^2$ [14].

[b] Following [14] the M^k parameters obtained from *ab initio* calculation [15] were used.

the new parameters and assignation, we repeated the above fitting procedure relaxing the AOM constrains step by step. The results are compiled in tables 4 and 5.

6. Discussion

As is seen in table 4 both models leave some lines unassigned. These are the lines at 8394 and 9490 cm^{-1} in the case of model (a) and the lines at 6458, 16 419 and 16 812 cm^{-1} in model (b). The three latter lines can be accounted for by the presence of U^{5+} and U^{3+} impurities. The presence of the U^{5+} lines in the absorption spectra of the uranium doped in zircon, hafnon and thorite has been confirmed by the angular dependence of the polarized transverse Zeeman spectra [17]. Using the AOM-I parametrization scheme we have found that two U^{5+} lines at 6700 and 9026 cm^{-1} observed for zircon by Vance and Mackey [17] correspond to $e_\sigma = 856$ cm^{-1} and $\zeta = 1965$ cm^{-1} and that the transitions have been of $\Gamma_7 \rightarrow \Gamma_7$ type. These data may be converted to the following energy pattern for U^{5+} in $UGeO_4$ (cm^{-1}): 0 (Γ_6), 821 (Γ_6), 858 (Γ_7), 6870 (Γ_6), 7253 (Γ_6), 8059 (Γ_7). The line at 6458 cm^{-1} observed in $UGeO_4$ may correspond to the simulated, 0 (Γ_6) → 6870 (Γ_6), model transition.

The peak at 8394 cm^{-1} is very weak and could be omitted, but on the other hand the intensity of the corresponding thermally induced transition is relatively high (see figure 1). This situation is well described in model (b). Attribution of the line to $\Gamma_1 \rightarrow \Gamma_3$ transition, which is forbidden in the case of D_{2d} symmetry but not in S_4, explains its low intensity in contrast to the corresponding transition from the thermally populated first excited Γ_5 level, allowed in both symmetries.

The line at 9490 cm^{-1} may be considered as a phonon-assisted transition corresponding to the zero-phonon line at 9070 cm^{-1} and the phonon frequency 420 cm^{-1}. Such a phonon energy has been shown to be associated with the stretching of cation–anion bonds [13]. The

intensity, however, is higher than that of other observed transitions of this type. Therefore, a coincidence with the electronic transition assumed in model (b) cannot be excluded.

As seen from table 5, the spectroscopic parameters in model (b) are determined much more precisely than in model (a). As a rule, the free-ion parameters do not differ much from the initial values except the P^2 parameters and perhaps the F^6 parameter in model (a) and the spin–orbit coupling constant ζ in model (b). Obviously, the similarity of the initial and final crystal-field parameters is less pronounced in model (a) where the starting parameters have been taken from another crystal, although the sign of all the parameters is preserved. In model (b) the B_0^6 parameter is the only one modified substantially by the fitting. The same parameter has been changed markedly in the *ab initio* calculations in relation to the crude AOM estimation (see table 2).

The two models differ significantly in the lowest part of the energy spectrum, which should have a considerable impact on the magnetic and thermodynamic properties. In fact, we have checked that the anisotropic low-temperature paramagnetic susceptibility has a maximum along the S_4 axis in model (b) and a minimum in model (a). Unfortunately, the difference between the models in the temperature dependence of the magnetic susceptibility and other thermodynamic quantities calculated for powder is much less apparent. Further experiments on single crystals are necessary to explain the doubts raised in this report.

Acknowledgments

We thank Dr P Porcher for creating a friendly and inspiring atmosphere during measurements in his laboratory and Dr S Hubert for valuable discussions concerning vibronic bands and providing us with unpublished spectroscopic data on thorium germanate matrices. One of us (ZG) gratefully acknowledges the support received from the Institut National de Physique Nucléaire et de Physique des Particles.

References

[1] Poirot I S, Kot W K, Edelstein N M, Abraham M M, Finch C B and Boatner L A 1989 *Phys. Rev.* B **39** 6388
[2] Khan Malek C and Krupa J C 1986 *J. Chem. Phys.* **84** 6584
[3] Krupa J C 1987 *Inorg. Chim. Acta.* **139** 223
[4] Kern S, Loong C K, Goodman G L, Crot B and Lander G H 1990 *J. Phys.: Condens. Matter* **2** 1933
[5] Krupa J C unpublished data
[6] Gajek Z and Mulak J 1992 *J. Phys.: Condens. Matter* **4** 947
[7] Gajek Z, Mulak J and Faucher M 1987 *J. Phys. Chem. Solids.* **48** 947
[8] Durif A 1956 *Acta Crystallogr.* **9** 533
[9] Reynolds K W, Boatner L A, Finch C B, Chatelain A and Abraham M M 1972 *J. Chem. Phys.* **56** 5607
[10] Ennaciri A, Kahn A and Michel D 1986 *J. Less-Common Met.* **124** 105
[11] Taylor M and Ewing R C 1978 *Acta Crystallogr.* B **34** 1074
[12] Gajek Z, Lahalle M P, Krupa J C and Mulak J 1988 *J. Less-Common Met.* **139** 351
[13] Vandenborre M T, Michel D and Ennaciri A 1989 *Spectrochim. Acta* **45A** 721
[14] Carnall W T, Liu G K, Williams C W and Reid M F 1991 *J. Chem. Phys.* **95** 7194
[15] Carnall W T and Crosswhite H M 1986 *The Chemistry of the Actinide Elements* 2nd edn, ed J J Katz, G T Seaborg and L R Morss (London: Chapman and Hall) p 1155
[16] Gajek Z, Mulak J and Krupa J C 1993 *J. Solid State Chem.* **107** at press
[17] Vance E R and Mackey D J 1978 *Phys. Rev.* **18** 185